J. Fluid Mech. (2010), *vol.* 649, *pp.* 497–508.
doi:10.1017/S0022112010000509

Maximum efficiency of wind turbine rotors using Joukowsky and Betz approaches

V. L. OKULOV† AND J. N. SØRENSEN

Department of Mechanical Engineering and Center for Fluid Dynamics, Technical University of Denmark, Nils Koppels Allé, 403, DK-2800 Lyngby, Denmark

(Received 18 September 2009; revised 26 January 2010; accepted 27 January 2010)

On the basis of the concepts outlined by Joukowsky nearly a century ago, an analytical aerodynamic optimization model is developed for rotors with a finite number of blades and constant circulation distribution. In the paper, we show the basics of the new model and compare its efficiency with results for rotors designed using the optimization model of Betz.

1. Introduction

In the history of rotor aerodynamics two 'schools' have dominated the conceptual interpretation of the optimum rotor. In Russia, Joukowsky (1912–1918) defined the optimum rotor as one having constant circulation along the blades, such that the vortex system for an N_b-bladed rotor consists of N_b helical tip vortices of strength Γ and an axial hub vortex of strength $-N_b\Gamma$. A simplified model of this vortex system can be obtained by representing it by a rotating horseshoe vortex (see figure 1*a*). The other school, which essentially was formed by Prandtl and Betz (see Betz 1919), assumed that optimum efficiency is obtained when the distribution of circulation along the blades generates a rigidly helicoidal wake that moves in the direction of its axis with a constant velocity. Betz used a vortex model of the rotating blades based on the lifting-line technique of Prandtl in which the vortex strength varies along the wingspan (figure 1*b*). This distribution, usually referred to as the Goldstein circulation function, is rather complex and difficult to determine accurately (Goldstein 1929). In both cases only conceptual ideas were outlined for rotors with finite number of blades, whereas later theoretical works mainly concerned actuator disk theory. Hence, in practice, the blades are modelled using blade–element momentum (BEM) theory, corrected by the tip correction of Prandtl (see e.g. Glauert 1935).

Recently, in Okulov & Sørensen (2008*a*, 2008*b*), we have derived an analytical solution for rotors with Goldstein distributions of circulation along the blade (Betz rotor) using a new analytical model of the velocity field induced by helical vortices (Okulov 2004). In the present work we exploit the analytical model further to develop a vortex theory of an ideal rotor based on the concepts outlined by Joukowsky using constant circulation along the blades (Joukowsky rotor). Both solutions enable for the first time to compare the theoretical maximum efficiency of wind turbines with Betz and Joukowsky rotors.

† Email address for correspondence: vaok@mek.dtu.dk

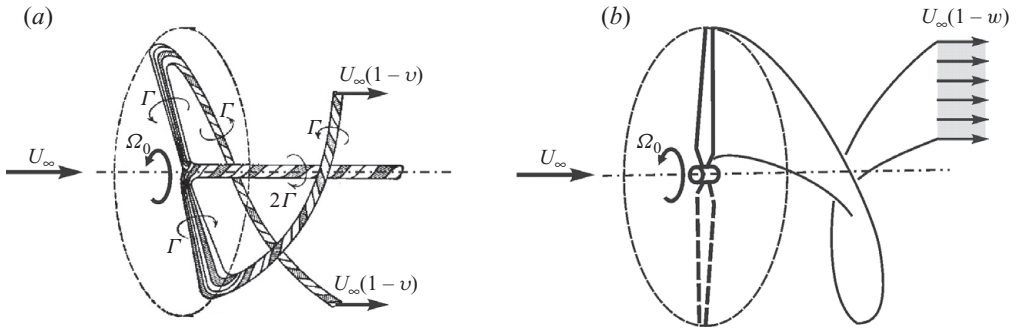

FIGURE 1. Sketch of the vortex system corresponding to lifting line theory of the ideal propeller of (*a*) Joukowsky and (*b*) Betz.

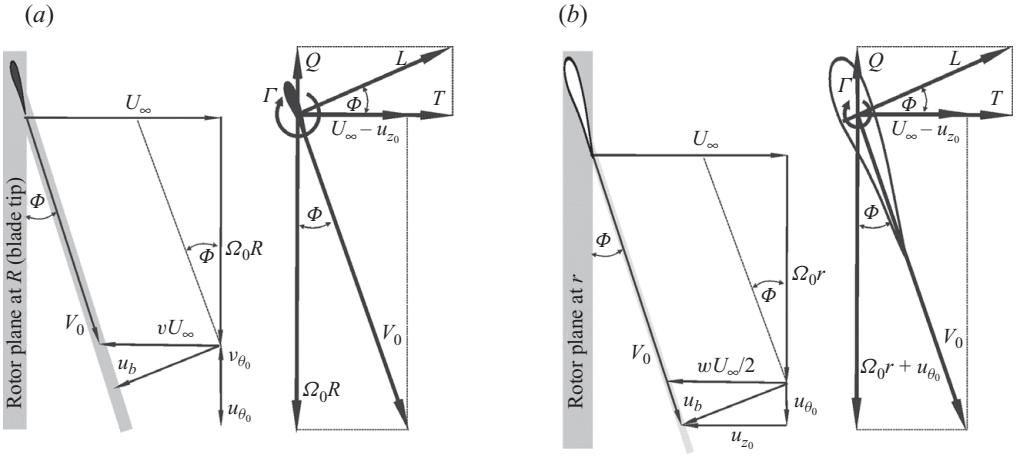

FIGURE 2. Velocity and power triangles in the rotor plane of (*a*) Joukowsky rotor and (*b*) Betz rotor.

2. Vortex theory for rotors with a finite number of blades

In the vortex theory, each of the blades is replaced by a lifting line on which the radial distribution of bound vorticity is represented by the circulation $\Gamma = \Gamma(r)$, which is a function of the radial distance along the rotor blade. This results in a free vortex system consisting of helical trailing vortices, as sketched in figures 1(*a*) and 1(*b*). Using the vortex theory, the bound vorticity serves to produce the local lift on the blades while the trailing vortices induce the velocity field in the rotor plane and the wake. As illustrated in figure 2 the velocity vector in the rotor plane is made up by the rotor angular velocity Ω_0, the undisturbed wind speed U_∞, the axial and circumferential velocity components u_{z_0} and u_{θ_0}, respectively, induced at a blade element in the rotor plane by the tip vortices, and v_{θ_0}, the circumferential velocity induced by the hub vortex. The fundamental expressions for the forces acting on a blade (figure 2) is most conveniently expressed by the Kutta–Joukowsky theorem, which in vector form reads

$$\mathrm{d}\boldsymbol{L} = \rho \boldsymbol{V}_0 \times \boldsymbol{\Gamma}\, \mathrm{d}r, \tag{1}$$

where $\mathrm{d}L$ is the lift force on a blade element of radial dimension $\mathrm{d}r$, V_0 is the resultant relative velocity and ρ is the density of the air. From (1), we can write the local torque

$\mathrm{d}Q$ of a rotor blade as follows:

$$\mathrm{d}Q = \rho\, \Gamma\, (U_\infty - u_{z_0})\, r\, \mathrm{d}r. \tag{2}$$

Integrating (2) along the blades and summing up, we get the following expression for the power output, $P = \Omega_0 Q$:

$$P = \rho N_b\, \Omega_0 \int_0^R \Gamma (U_\infty - u_{z_0})\, r\, \mathrm{d}r, \tag{3}$$

where R is the radius of the rotor.

To determine the theoretical maximum efficiency of a rotor, the power coefficient is introduced as follows:

$$C_P = P/\left(\tfrac{1}{2}\rho\pi R^2 U_\infty^3\right). \tag{4}$$

The maximum power that can be extracted from a stream of air contained in an area equivalent to that swept out by the rotor corresponds to the maximum value of the power coefficient. This is determined as a function of the tip speed ratio

$$\lambda_0 = \Omega_0 R / U_\infty. \tag{5}$$

To determine the velocity field v_{θ_0}, u_{z_0} and u_{θ_0} induced at a blade element in the rotor plane, the free half-infinite helical vortex system behind the rotor is replaced by 'an associated vortex system' that extends to infinity in both directions. Neglecting deformations or changes in the wake, the vortex system is uniquely described by the far wake properties in the so-called Trefftz plane, which per definition is the plane normal to the relative wind far downstream of the rotor. Thus, in accordance with Helmholtz' vortex theorem, the bound circulation Γ about a blade element is uniquely related to the circulation of a corresponding vortex in the Trefftz plane. By symmetry, it is readily seen that the induced velocities at a point in the rotor plane (figure 2) equals half the induced velocity at a corresponding point in the Trefftz plane (see e.g. Joukowsky 1912–1918; Betz 1919):

$$v_{\theta_0} = \tfrac{1}{2} v_\theta, \quad u_{\theta_0} = \tfrac{1}{2} u_\theta \quad \text{and} \quad u_{z_0} = \tfrac{1}{2} u_z. \tag{6}$$

3. Solution of Joukowsky rotor

In the vortex theory of the Joukowsky rotor (Joukowsky 1912–1918), each of the blades is replaced by a lifting line about which the circulation associated with the bound vorticity is constant, resulting in a free vortex system consisting of helical vortices trailing from the tips of the blades and a rectilinear hub vortex. The vortex system may be interpreted as consisting of rotating horseshoe vortices with cores of finite size, as sketched in figure 1(*a*) which is reproduced from the original drawing of Joukowsky. The 'associated vortex system' consists of a multiplet of helical tip vortices of finite vortex cores ($\varepsilon \ll R$) with constant pitch h and circulation Γ. The multiplet moves downwind (in the case of a propeller) or upwind (in the case of a wind turbine) with a constant velocity $U_\infty(1 \pm \upsilon)$ in the axial direction where υ denotes the difference between the wind speed and axial translational velocity of the vortices. Denoting the angle between the axis of the tip vortex and the Trefftz plane as Φ (see figure 2*a*), the helical pitch of the multiplet is given as

$$h = 2\pi R \tan\Phi \quad \text{or} \quad l/R = h/2\pi R = \tan\Phi. \tag{7}$$

The free vortex lines are made up by vortex cores of finite size in order to avoid singular behaviour. The vortex cores are collinear to the axes of the helical lines

and their vorticity is assumed to be uniform and densely distributed across the core cross-section. According to Okulov (2004), in cylindrical coordinates (r, θ, z), the components of fluid velocity induced by N_b helical vortices in the domain outside the vortex cores are given as

$$u_z(r,\chi) = \frac{N_b\Gamma}{2\pi l}\left\{\begin{matrix}1\\0\end{matrix}\right\} - \frac{\Gamma R}{\pi l^2}\sum_{n=1}^{N_b}\sum_{m=1}^{\infty} m\left\{\begin{matrix}I_m(mr/l)K'_m(mR/l)\\I'_m(mR/l)K_m(mr/l)\end{matrix}\right\}\cos(m\chi_n), \tag{8}$$

$$u_\theta(r,\chi) = \frac{N_b\Gamma}{2\pi r}\left\{\begin{matrix}0\\1\end{matrix}\right\} + \frac{\Gamma R}{\pi r l}\sum_{n=1}^{N_b}\sum_{m=1}^{\infty} m\left\{\begin{matrix}I_m(mr/l)K'_m(mR/l)\\I'_m(mR/l)K_m(mr/l)\end{matrix}\right\}\cos(m\chi_n), \tag{9}$$

where $I_m(x)$ and $K_m(x)$ are modified Bessel functions; $\chi = \theta - (z/l)$ and $\chi_n = \chi + (2\pi(n-1)/N_b)$. When the first two dominant singularity terms are extracted, (8) and (9) are reduced to the following rough-and-ready formulae (Fukumoto & Okulov 2005):

$$u_z(r,\chi) = \frac{\Gamma}{2\pi l}\left(\left\{\begin{matrix}N_b\\0\end{matrix}\right\} + \frac{\sqrt[4]{l^2+R^2}}{\sqrt[4]{l^2+r^2}}\sum_{n=1}^{N_b} Re\left[\frac{\pm e^{i\chi_n}}{e^{\mp\xi} - e^{i\chi_n}} + \frac{l}{24}\left(\frac{3r^2-2l}{(l^2+r^2)^{3/2}} + \frac{3R^2-2l}{(l^2+R^2)^{3/2}}\right)\ln(1-e^{\xi+i\chi_n})\right]\right), \tag{10}$$

$$u_\theta(r,\chi) = \frac{\Gamma}{2\pi r}\left(\left\{\begin{matrix}0\\N_b\end{matrix}\right\} - \frac{\sqrt[4]{l^2+R^2}}{\sqrt[4]{l^2+r^2}}\sum_{n=1}^{N_b} Re\left[\frac{\pm e^{i\chi_n}}{e^{\mp\xi} - e^{i\chi_n}} + \frac{l}{24}\left(\frac{3r^2-2l}{(l^2+r^2)^{3/2}} + \frac{3R^2-2l}{(l^2+R^2)^{3/2}}\right)\ln(1-e^{\xi+i\chi_n})\right]\right), \tag{11}$$

where

$$e^{\xi} = \frac{r\left(1+\sqrt{1+R^2/l^2}\right)\exp\left(\sqrt{1+r^2/l^2}\right)}{R\left(1+\sqrt{1+r^2/l^2}\right)\exp\left(\sqrt{1+R^2/l^2}\right)}$$

(unfortunately, this expression was printed with an error in articles by Fukumoto & Okulov 2005 and Okulov & Sørensen 2008*a*, 2008*b*). Here we use notations '$\pm$' and '$\{:\}$', in which the upper sign or symbols in brackets correspond to $r < R$ and the lower to $r \geqslant R$. The velocity component in the χ-direction is given as (Okulov 2004)

$$u_\chi = u_\theta - \frac{r}{l}u_z. \tag{12}$$

Introducing the azimuthally averaged induced axial velocity as $\langle u_z\rangle_\theta = (\int_0^{2\pi} u_z \mathrm{d}\theta)/2\pi$, from (8) we get

$$\langle u_z\rangle_\theta = 0 \quad \text{for} \quad r > R \quad \text{and} \quad \langle u_z\rangle_\theta = \frac{N_b\Gamma}{2\pi l} \equiv const \quad \text{for} \quad r < R. \tag{13}$$

Note that the dimensionless averaged induced axial velocity in the wake ($0 < r < R$), which is identical to the total axial wake interference factor a, takes the same constant value

$$aU_\infty \equiv \langle\langle u_z\rangle_\theta\rangle_{0<r<R} = \frac{N_b\Gamma}{2\pi l}. \tag{14}$$

The vortex system also includes a rectilinear hub vortex of strength $-N_b\Gamma$, resulting in a simple formula for the additional induced velocity that only consists of the

circumferential component

$$v_\theta = -\frac{N_b \Gamma}{2\pi r}. \tag{15}$$

Defining the azimuthally averaged azimuthal velocity induced by the helical multiplet as $\langle u_\theta \rangle_\theta = (\int_0^{2\pi} u_\theta \mathrm{d}\theta)/2\pi$, and combining (9) and (15), we get

$$v_\theta|_{r=R} = -\langle u_\theta \rangle_\theta|_{r=R}\,. \tag{16}$$

To eliminate the singularity of the induced velocity field in the vicinity of the vortex filament, the vortex system is represented by a set of helical vortices with finite core. For an unexpanded wake originating from a rotor with infinitely many blades, the convective velocity of the vortex system equals half the averaged induced axial velocity in the wake. This is sometimes referred to as the 'roller-bearing analogy'. Although this approximation cannot be rigorously justified for a vortex system consisting of a finite number of vortices, we employ the same analogy by assuming that the helical vortices are transported with a relative axial speed, υ, that corresponds to half the averaged induced velocity:

$$\upsilon = \frac{1}{2} a \frac{(R+\varepsilon)}{R}, \tag{17}$$

where a correction of small expansion of the cross-section of the wake is made in order to include the radius ε of the vortex cores. Thus, the vortices are assumed to translate in the bi-normal direction to the helical axis of the tip vortices with the velocity u_b (figure 2*a*):

$$u_b \equiv \upsilon \cos\Phi = \frac{a(R+\varepsilon)}{2R}\cos\Phi \equiv \frac{a(R+\varepsilon)}{2R}\frac{R}{\sqrt{R^2+l^2}}. \tag{18}$$

The problem of determining the induced equilibrium motion of a multiple of helical vortices in an unbounded domain was solved by Okulov (2004), but here we will use a more suitable notation introduced by Okulov & Sørensen (2007). The motion of the tip vortices in the χ-direction can be described by (2.13) of Okulov & Sørensen (2007) in the form

$$\begin{aligned}\frac{4\pi R}{\Gamma} u_\chi(\sigma) \equiv \bar{u}_\chi(\sigma) = &-\frac{\sqrt{1+\tau^2}}{\tau} - \frac{N_b}{\tau^2} + \frac{1}{\tau(1+\tau^2)^{1/2}} \\ &\times \left(\ln \frac{\sigma N_b (1+\tau^2)^{3/2}}{\tau} + \frac{1}{4}\right) - \frac{\tau}{(1+\tau^2)^{7/2}}\left(\tau^4 - 3\tau^2 + \frac{3}{8}\right)\frac{\zeta(3)}{N_b^2},\end{aligned} \tag{19}$$

where $\tau = l/R$ and $\sigma = \varepsilon/R$ are the non-dimensional pitch and radius of the vortex core, respectively, and $\zeta(3) = 1.20206\ldots$ is the Riemann zeta function. Introducing the bi-normal velocity component, u_b, as

$$u_b = -u_\chi \frac{l}{\sqrt{R^2+l^2}}, \tag{20}$$

the conditions for equilibrium motion of the far wake are now determined in accordance with the 'roller-bearing analogy' of (18). Finally, for this wake motion the dimensionless radius σ of the tip vortex core must satisfy the equation

$$\bar{u}_\chi(\sigma) = -\frac{N_b}{\tau^2}(1+\sigma). \tag{21}$$

For any given value of pitch l and number of rotor blades N_b, we compute the radius of the tip vortex core by solving (21). Figure 3(*a*) shows the 'total' core size, which is

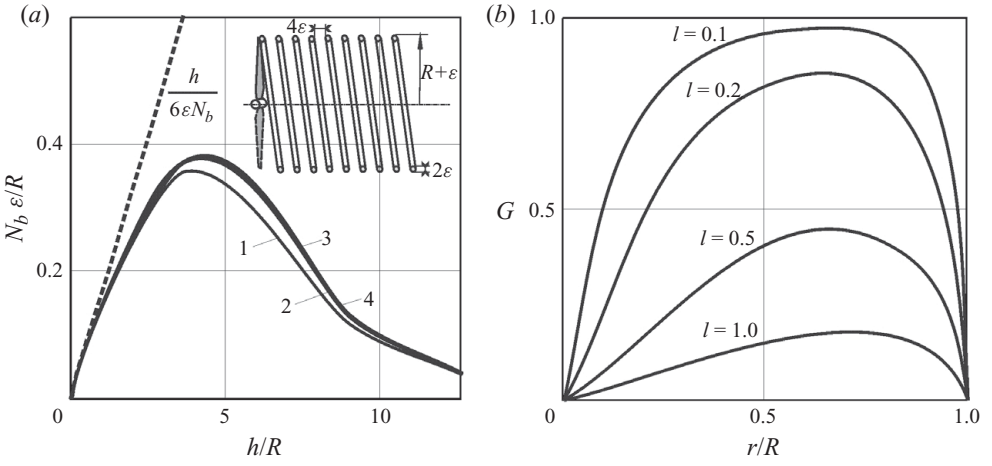

FIGURE 3. (*a*) Joukowsky rotor. The vortex core radius for equilibrium motion of tip vortex multiplet as a function of helical pitch for different numbers of blades (here and hereby in the next figures, the number on the solid line curves refer to the number of blades); dotted line indicates asymptotic behaviour of the core radius for small pitch and the sketch shows the helical tip vortices representing the limit case of the wake. (*b*) Betz rotor. Examples of Goldstein function for three blades and different values of helical pitch.

equal to the vortex core radius multiplied by the number of blades, as a function of the tip vortex pitch for different number of blades. It may be noted that the limit of small pitch has the same asymptote for all number of blades and the 'total' core tends to zero faster than the pitch with a fixed ratio $h/N_b\varepsilon = 6$. This implies that the distance between the tip vortices, independent of the value of the pitch, is always greater than 4 core radii, as depicted in figure 3. This also implies that it is impossible to reach a dense cylindrical vortex surface as used in the actuator disk theory. In the other limit, when the pitch tends to infinity, the vortex core disappears, which shows that an equilibrium vortex multiplet motion is achieved when the vortices become rectilinear.

The axial velocity field induced by the tip vortices can subsequently be determined in all points of the Trefftz plane because we have defined the finite radius of the tip vortex core by the 'roller-bearing analogy'. The velocities outside the vortices are determined by (8) and inside the vortex cores by taking the average value of the velocity on the boundary of the vortex cores. The axial velocity, made dimensionless with the azimuthally averaged induced axial velocity $\langle u_z\rangle_\theta$ of (13) in the n-blade direction ($\theta = 2\pi n/N_b$, $z = 0$), takes the form:

$$\tilde{u}_z\left(r, \frac{2\pi n}{N_b}\right) = \frac{1}{aU_\infty}\begin{cases} u_z\left(r, \dfrac{2\pi n}{N_b}\right) & \text{if} \quad r < R-\varepsilon \quad \text{and} \quad r > R+\varepsilon, \\ \dfrac{R+\varepsilon-r}{2\varepsilon}u_z\left(R-\varepsilon, \dfrac{2\pi n}{N_b}\right) - \dfrac{R-\varepsilon-r}{2\varepsilon}u_z\left(R+\varepsilon, \dfrac{2\pi n}{N_b}\right) & \\ \qquad\qquad \text{if} \quad R-\varepsilon < r < R+\varepsilon. \end{cases} \tag{22}$$

From (14), we get the following relation between the bound circulation and the interference factor:

$$N_b\Gamma = 2\pi\, l a U_\infty. \tag{23}$$

From simple geometric considerations in the rotor plane (figure 2*a*), using (16) and (17), the angular pitch is given as

$$\tan\Phi|_{r=R} = \frac{U_\infty - |u_{z_0}|_{r=R}}{\Omega_0 R + |u_{\theta_0}|_{r=R} - |v_{\theta_0}|_{r=R}} = \frac{U_\infty(1-\upsilon)}{\Omega_0 R} = \frac{U_\infty\left[1-\frac{1}{2}a(1+\sigma)\right]}{\Omega_0 R} = \tau \equiv \frac{l}{R}. \tag{24}$$

Equation (24) can be also written as

$$\Omega_0 l = U_\infty - \tfrac{1}{2}aU_\infty(1+\sigma). \tag{25}$$

Inserting (6), (22), (23) and (25) into (3), the power can be determined from the following integral:

$$P = \rho\,\pi R^2\,U_\infty^3 a\left(1-\frac{a}{2}(1+\sigma)\right)\left(1-a\int_0^1 \tilde{u}_z(x,0)\,x\,\mathrm{d}x\right). \tag{26}$$

Performing the integration and introducing the dimensionless power coefficient (4), we get

$$C_P = 2a\left(1-\tfrac{1}{2}a\,J_1\right)\left(1-\tfrac{1}{2}a\,J_3\right), \tag{27}$$

where $J_1 = 1+\sigma$ and $J_3 = 2\int_0^1 \tilde{u}_z(x,0)x\mathrm{d}x$. For a given helicoidal wake structure, the power coefficient is seen to be uniquely determined, except for the parameter a. Differentiation of C_P with respect to a yields the maximum value, $C_{P,max}$, resulting in

$$a(C_P = C_{P,max}) = \frac{2}{3J_1J_3}\left(J_1 + J_3 - \sqrt{J_1^2 - J_1J_3 + J_3^2}\right). \tag{28}$$

4. Solution of the Betz rotor

To compare the efficiency of the Joukowsky rotor with the Betz rotor, we here outline the main points of the derivation of the aerodynamics of the Betz rotor (for more details we refer to Okulov & Sørensen 2008*a*). In this model, which is based on Lanchester–Prandtl wing theory, the vortex strength of the lifting line varies along the blade span, following the so-called Goldstein distribution. This results in a vortex sheet that is continuously shed from the trailing edge (figure 1*b*). Betz (1919) showed that the ideal efficiency is obtained when the distribution of circulation along the blade produces a rigidly moving helicoidal vortex sheet with constant pitch, h, that moves downwind (in the case of a propeller) or upwind (in the case of a wind turbine) in the axial direction of its axis with a constant velocity $U_\infty(1 \pm w)$. 'The associated vortex system' to the wake consists of a regular helical sheet extended to infinity in both directions. Denoting the angle between the vortex sheet and the Trefftz plane as Φ (see figure 2*b*), the pitch is given as

$$h = 2\pi r\tan\Phi \quad \text{or} \quad l/r = h/2\pi r = \tan\Phi, \tag{29}$$

where r is the radial distance along the sheet. Since the sheet is translated with constant relative axial speed wU_∞, the induced velocity comprises only the component $wU_\infty\cos\Phi$ that is 'pushed' normal to the screw surface (figure 2*b*). The axial and circumferential velocity components u_z and u_θ induced by the infinite sheet at the sheet itself are therefore given as

$$u_\theta = wU_\infty\cos\Phi\sin\Phi \quad \text{and} \quad u_z = wU_\infty\cos^2\Phi. \tag{30}$$

From simple geometric considerations these equations are rewritten as

$$u_\theta = wU_\infty \frac{xl}{l^2+x^2} \quad \text{and} \quad u_z = wU_\infty \frac{x^2}{l^2+x^2}, \tag{31}$$

where $x = r/R$ is the dimensionless radius.

Goldstein (1929) was the first who found an analytical solution to the potential flow problem of the moving 'associated vortex system' consisting of an infinite helical vortex sheet. In his model a dimensionless distribution $G(x,l)$ of circulation was introduced as follows:

$$N_b\Gamma(x,l) = 2\pi l\, wU_\infty G(x,l). \tag{32}$$

Using infinite series of Bessel functions, Goldstein (1929) succeeded in obtaining an analytical solution to the problem, but for $N_b = 2$ and 4 only. For any given value of the wake pitch l and number of rotor blades N_b, the Goldstein circulation function $G(x,l)$, shown in figure 3(*b*), has been determined by Okulov & Sørensen (2008*a*, 2008*b*).

To compute the power coefficient, we employ the same procedure as outlined in the previous section, that is we integrate (3) using (6), and the lift distribution in (32). In addition to this, from geometric considerations in the rotor plane (figure 2*b*), using (29) and (30), the angular pitch is given as (a derivation of this relation is shown in the Appendix)

$$\tan\Phi = \frac{U_\infty - \frac{1}{2}u_z}{\Omega_0 r + \frac{1}{2}u_\theta} = \frac{U_\infty\left(1-\frac{1}{2}w\right)}{\Omega_0 r} = \frac{l}{r}. \tag{33}$$

Equation (33) can also be written as

$$\Omega_0 l = U_\infty\left(1-\tfrac{1}{2}w\right). \tag{34}$$

Inserting (31), (32) and (34) into (3), the power can be determined from the following integral:

$$P = \rho\pi R^2 U_\infty^3 w\left(1-\frac{w}{2}\right)\int_0^1 2G(x,l)\left(1-\frac{w}{2}\frac{x^2}{x^2+l^2}\right)x\,\mathrm{d}x. \tag{35}$$

Performing the integration and introducing the dimensionless power coefficient (see (4)), we get

$$C_P = 2w\left(1-\tfrac{1}{2}w\right)\left(I_1 - \tfrac{1}{2}wI_3\right), \tag{36}$$

where

$$I_1 = 2\int_0^1 G(x,l)\,x\,\mathrm{d}x \quad \text{and} \quad I_3 = 2\int_0^1 G(x,l)\frac{x^3\,\mathrm{d}x}{x^2+l^2}.$$

The coefficients I_1 and I_3 are usually referred to as the mass coefficient and the axial energy factor, respectively. For a given helicoidal wake structure, the power and thrust coefficients are seen to be uniquely determined, except for the parameter w. Differentiation of C_P (see (36)) with respect to w yields the maximum value, $C_{P,max}$, resulting in

$$w(C_P = C_{P,max}) = \frac{2}{3I_3}\left(I_1 + I_3 - \sqrt{I_1^2 - I_1 I_3 + I_3^2}\right). \tag{37}$$

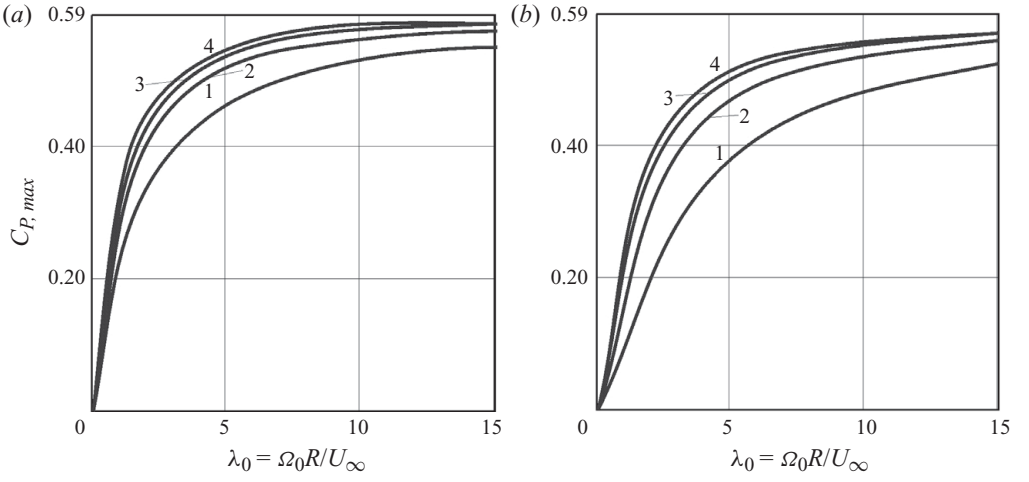

FIGURE 4. Power coefficients, C_P, of an optimum rotor as a function of tip speed ratio and number of blades. (*a*) Joukowsky rotor and (*b*) Betz rotor.

5. Results and discussion

In the following we present some representative results from the new model. To compare the performance of rotors of constant circulation (Joukowsky rotor) with rotors optimized using the Goldstein circulation distribution, we show results from both models. To compare the efficiency of the two rotor concepts it is needed to use some unambiguous parameters. As usual in rotor aerodynamics, we employ the axial interference factor a and the tip speed ratio λ_0. However, since a does not appear explicitly in (36) and (37) and λ_0 does not appear explicitly in any of the equations, it is needed to derive some additional relations. In the case of a Betz rotor, λ_0 is connected to the helical pitch l and the generic parameter w through (34), resulting in the following relationship:

$$\lambda_0 \equiv \frac{\Omega_0 R}{U_\infty} = \frac{R}{l}\left(1 - \frac{w}{2}\right). \tag{38}$$

For a Joukowsky rotor a similar dependency can be found from (25):

$$\lambda_0 \equiv \frac{\Omega_0 R}{U_\infty} = \frac{R}{l}\left(1 - \frac{a}{2}\left(1 + \frac{\varepsilon}{R}\right)\right). \tag{39}$$

Figure 4 presents the optimum power coefficient of both models for different number of blades as a function of tip speed ratio. From the plots it is evident that the optimum power coefficient of the Joukowsky rotor for all number of blades is larger than that for the Betz rotor. The difference, however, vanishes for $\lambda \to \infty$ or for $N_b \to \infty$, where both models tend towards the Betz limit.

In the Betz model, an expression for the axial interference factor can be obtained by combining (8) and (32) as

$$a = w \int_0^1 G(x, l)\,\mathrm{d}x. \tag{40}$$

In figure 5, we display the axial interference factor of the two rotors as a function of tip speed ratio and number of blades. Comparing the two plots, it is readily seen that the Betz rotor for the same tip speed ratio decelerates the flow less than

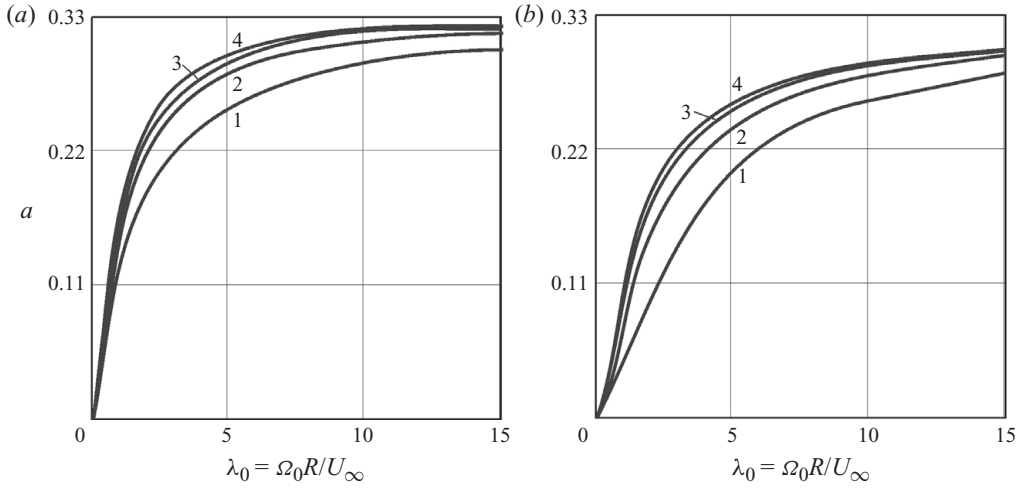

FIGURE 5. Axial interference factor as a function of tip speed ratio and number of blades. (*a*) Joukowsky rotor and (*b*) Betz rotor.

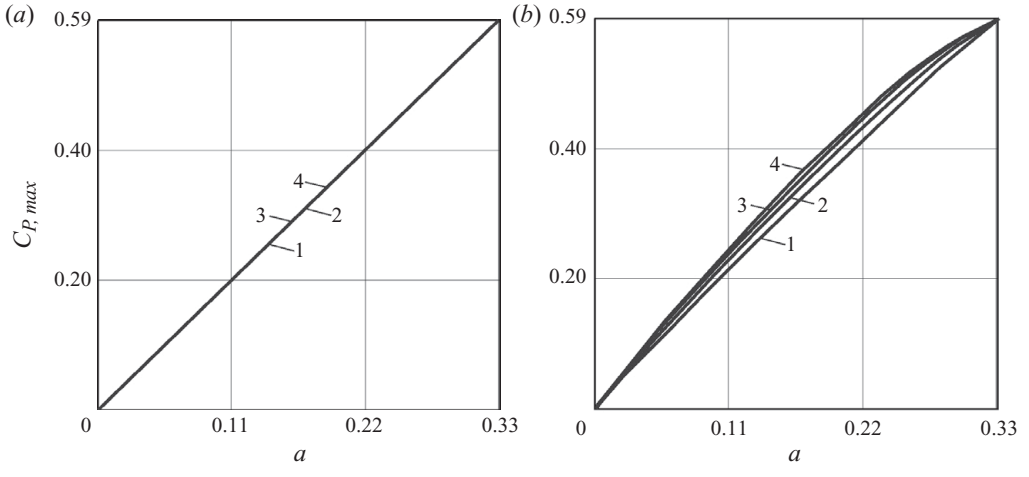

FIGURE 6. Power coefficient, C_P, of an optimum rotor as a function of axial interference factor and number of blades. (*a*) Joukowsky rotor and (*b*) Betz rotor.

the Joukowsky rotor. As a consequence, if we employ the axial interference factor as independent variable, an optimum Betz rotor can produce more power than a Joukowsky rotor under the same deceleration of the wind (see figure 6).

6. Conclusion

An analytical model has been developed for a rotor with a finite number of blades and constant circulation ('Joukowsky rotor'). The method is based on an analytical solution to the problem of equilibrium motion of a helical vortex multiplet in a far wake. The vortex system behind the rotor is represented by a set of helical vortices with finite core to eliminate the singularity of the induced velocity field in the vicinity of each filament. The finite core radius is determined in the framework of an ideal

fluid by assuming that the relative wake motion is governed by a constant axial speed equal to half the averaged induced velocity in the wake. The main achievement of the model is that it eliminates the singularity of the solution at all operating conditions. In contrast to earlier models, the new model enables for the first time to determine the theoretical maximum efficiency of rotors with constant circulation and an arbitrary number of blades.

Optimum conditions for finite number of blades as a function of tip speed ratio were compared for two models: (*a*) Joukowsky rotor with constant circulation along the blade, and (*b*) Betz rotor with circulation given by Goldstein's function. For all tip speed ratios the Joukowsky rotor achieves a higher efficiency than the Betz rotor, but the efficiency of the Betz rotor is larger if we compare it for the same deceleration of the wind speed.

Appendix

The relation given in (33) can be deduced as follows:

$$\tan\Phi = \frac{\sin\Phi}{\cos\Phi} = \frac{U_\infty - \frac{1}{2}u_z}{\Omega_0 r + \frac{1}{2}u_\theta} = \frac{U_\infty\left(1 - \frac{1}{2}w\cos^2\Phi\right)}{\Omega_0 r + \frac{1}{2}U_\infty w\cos\Phi\sin\Phi}$$

$$\Rightarrow \Omega_0 r\sin\Phi + \frac{1}{2}U_\infty w\cos\Phi\sin^2\Phi = U_\infty\cos\Phi\left(1 - \frac{1}{2}w\cos^2\Phi\right)$$

$$\Rightarrow \Omega_0 r\sin\Phi = U_\infty\cos\Phi\left(1 - \frac{1}{2}w(\cos^2\Phi + \sin^2\Phi)\right)$$

$$\Rightarrow \tan\Phi = \frac{\sin\Phi}{\cos\Phi} = \frac{U_\infty\left(1 - \frac{1}{2}w\right)}{\Omega_0 r}.$$

From which it follows that

$$\frac{U_\infty - \frac{1}{2}u_z}{\Omega_0 r + \frac{1}{2}u_\theta} = \frac{U_\infty\left(1 - \frac{1}{2}w\right)}{\Omega_0 r}.$$

REFERENCES

Betz, A. 1919 Schraubenpropeller mit geringstem Energieverlust. Dissertation, Göttingen Nachrichten, Göttingen.

Fukumoto, Y. & Okulov, V. L. 2005 The velocity field induced by a helical vortex tube. *Phys. Fluids.* **17** (10), 107101 (1–19).

Glauert, H. 1935 Airplane propellers. In *Division L in Aerodynamic Theory* (ed. Durand), vol. 4, pp. 169–360. Springer.

Goldstein, S. 1929 On the vortex theory of screw propellers. *Proc. R. Soc. Lond.* A **123**, 440–465.

Joukowsky, N. E. 1912 Vortex theory of screw propeller, I. *Trudy Otdeleniya Fizicheskikh Nauk Obshchestva Lubitelei Estestvoznaniya* **16** (1), 1–31 (in Russian). French translation in: *Théorie tourbillonnaire de l'hélice propulsive* (Gauthier-Villars, Paris, 1929) 1–47.

Joukowsky, N. E. 1914 Vortex theory of screw propeller, II. *Trudy Otdeleniya Fizicheskikh Nauk Obshchestva Lubitelei Estestvoznaniya* **17** (1), 1–33 (in Russian). French translation in: *Théorie tourbillonnaire de l'hélice propulsive* (Gauthier-Villars, Paris, 1929) 48–93.

Joukowsky, N. E. 1915 Vortex theory of screw propeller, III. *Trudy Otdeleniya Fizicheskikh Nauk Obshchestva Lubitelei Estestvoznaniya* **17** (2), 1–23 (in Russian). French translation in: *Théorie tourbillonnaire de l'hélice propulsive* (Gauthier-Villars, Paris, 1929) 94–122.

Joukowsky, N. E. 1918 Vortex theory of screw propeller, IV. *Trudy Avia Raschetno-Ispytatelnogo Byuro*, no 3, 1–97 (in Russian). French translation in: *Théorie tourbillonnaire de l'hélice propulsive* (Gauthier-Villars, Paris, 1929) 123–198.

Okulov, V. L. 2004 On the stability of multiple helical vortices. *J. Fluid Mech.* **521**, 319–342.

Okulov, V. L. & Sørensen, J. N. 2007 Stability of helical tip vortices in rotor far wake. *J. Fluid Mech.* **576**, 1–25.

Okulov, V. L. & Sørensen, J. N. 2008*a* Refined Betz limit for rotors with a finite number of blades. *Wind Energy* **11** (4), 415–426.

Okulov, V. L. & Sørensen, J. N. 2008*b* An ideal wind turbine with a finite number of blades. *Doklady Phys.* **53** (6), 337–342.